

## Phonon Hall Viscosity of Ionic Crystals

 B. Flebus<sup>1</sup> and A. H. MacDonald<sup>2</sup>
<sup>1</sup>*Department of Physics, Boston College, 140 Commonwealth Avenue Chestnut Hill, Massachusetts 02467, USA*
<sup>2</sup>*Physics Department, University of Texas at Austin, Austin, Texas 78712, USA*
 (Received 26 May 2022; revised 14 March 2023; accepted 6 November 2023; published 4 December 2023)

When time-reversal symmetry is broken, the low-energy description of acoustic lattice dynamics allows for a dissipationless component of the viscosity tensor, the phonon Hall viscosity, which captures how phonon chirality grows with the wave vector. In this work, we show that, in ionic crystals, a phonon Hall viscosity contribution is produced by the Lorentz forces on moving ions. We calculate typical values of the Lorentz force contribution to the Hall viscosity using a simple square lattice toy model, and we compare it with literature estimates of the strengths of other Hall-viscosity mechanisms.

DOI: 10.1103/PhysRevLett.131.236301

**Introduction.**—Recent measurements of giant thermal Hall signals in many insulating ionic crystals [1–5] have ignited widespread interest in the processes underlying chiral phonon transport. The mechanisms by which phonons acquire chirality can be broadly divided in two classes: (i) intrinsic—i.e., originating from external magnetic fields or magnetism that breaks time-reversal symmetry (TRS) in crystals [6–25], and (ii) extrinsic—i.e., originating from scattering on TRS-breaking crystal defects [26–29].

In the low-energy elasticity-theory description of acoustic waves, intrinsic TRS-breaking is accounted for by a Hall viscosity contribution to the response of the system’s viscoelastic stress tensor to an applied strain  $u_{\lambda\mu}$  [7,11]:

$$\langle \hat{T}_{\lambda\mu} \rangle = \Lambda_{\lambda\mu\nu\xi} u_{\nu\xi} + \eta_{\lambda\mu\nu\xi} \dot{u}_{\nu\xi}. \quad (1)$$

Here,  $\hat{T}$  is the stress tensor,  $u_{\lambda\mu} = \frac{1}{2}(\partial_\lambda u_\mu + \partial_\mu u_\lambda)$  is the strain tensor,  $u_\lambda$  is the atomic displacement field along the  $\lambda$ th direction, and  $\Lambda$  and  $\eta$  are, respectively, the elasticity and viscosity tensors. The viscosity tensor  $\eta$  can have dissipationless component, dubbed the Hall (or odd) viscosity, which is associated with the part of  $\eta_{\lambda\mu\nu\xi}$  that is antisymmetric under exchange of the pairs of indices  $(\lambda\mu)$  and  $(\nu\xi)$ .

Dissipationless Hall contributions to the viscosity [7] are allowed only in systems with broken TRS where they alters the acoustic phonon spectrum, and mix longitudinal and transverse modes. Previous theoretical work has addressed phonon Hall viscosities produced by coupling of acoustic phonons to a ferroelectric [6], electronic [7–10,12–15], or spin environment [16–25] in which TRS is broken.

In this Letter, we consider the role of Lorentz forces in ionic crystals, which act on the electric dipoles produced by out-of-phase motion of cations and anions. The out-of-phase lattice vibrations are, in turn, coupled at finite wave vector to the in-phase modes by elastic forces. By deriving

an effective theory for the low-energy acoustic waves, we show that Lorentz forces always lead to finite Hall viscosities that are linear in magnetic field.

The Lorentz-force Hall effect mechanism identified in this Letter must be present in any ionic crystal and is readily

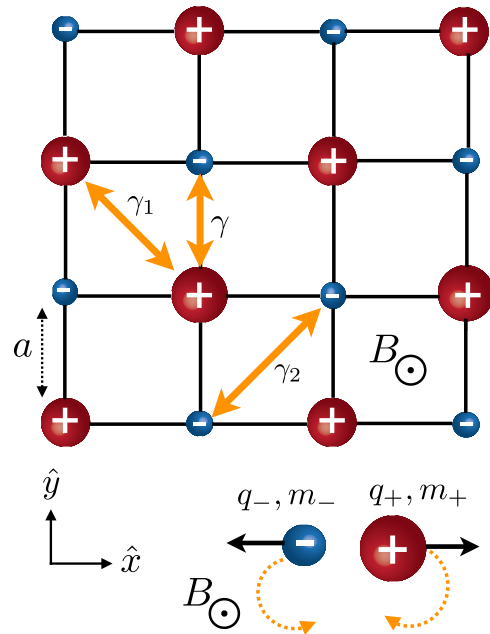


FIG. 1. Top: Diatomic square lattice with interatomic distance  $a$ , subjected to an out-of-plane magnetic field  $B$ . The cation and anion masses are  $m_+$  and  $m_-$ , and the ion effective charges are  $q_\pm = \pm Z^* e$ . We include centrosymmetric pairwise interactions between ions characterized by spring constants  $\gamma$ ,  $\gamma_1$ , and  $\gamma_2$  for near-neighbor interactions between cations and anions, second-neighbor interactions cations, and second-neighbor interactions between anions, respectively. Bottom: optical modes in an ionic crystal. In the presence of a magnetic field  $B$  perpendicular to the  $2d$  crystalline plane, the Lorentz forces on cations and anions moving in opposite directions do not cancel.

evaluated for particular materials given a set of lattice force constants and ionic charges. In order to bring out the mechanisms that control Hall viscosity trends across materials, we analyze a two-dimensional model. Specifically, we focus on the diatomic square lattice subjected to an out-of-plane magnetic field, sketched in Fig. 1, to estimate the typical size of contributions to the Hall viscosity tensor  $\eta$  supplied by this mechanism. Because of the  $C_4$  rotational symmetry of our  $2d$  model, there is only one independent coefficient in the phonon Hall viscosity tensor, i.e.,  $\eta^H = \eta_{xxxy}$  [30]. We find that this coefficient is proportional to the external magnetic field, and that its typical numerical value is comparable to those estimated for other mechanisms. Our results show that every ionic crystal can display a phonon Hall response, independently of phonon coupling to external degrees of freedom. Furthermore, our discovery sheds further light on the mechanisms underlying the generation of phonon chirality and angular momentum in ionic insulators, which have been recently attracting significant attention across different fields in condensed matter physics and nonlinear optics [31–38].

*Model.*—We consider a square lattice with cations and anions on opposite sublattices that is subjected to an out-of-plane magnetic field  $B$ , as depicted in Fig. 1. The cation and anion have masses  $m_+$  and  $m_-$  and charges  $q_{\pm} = \pm Z^*e$ , respectively, with  $e > 0$  being the electron charge and  $Z^*$  the effective ionic charge number. We assume centrosymmetric forces with spring constants  $\gamma$ ,  $\gamma_1$ , and  $\gamma_2$  for interactions between cation and anion nearest neighbors, cation second nearest neighbors, and anion second nearest neighbors, respectively.

At wave vector  $\mathbf{k}$ , the lattice displacement along the  $i$ th direction of the  $n$ th ion (with  $n = \pm$ ) in the  $l$ th cell can be written as

$$u_{n\mu l}(\mathbf{k}, \omega) = m_n^{-1/2} u_{n\mu} e^{i\mathbf{k} \cdot \mathbf{R}_n(l) - i\omega t}. \quad (2)$$

Here,  $u_{n\mu}$  is the lattice vibration amplitude of the  $n$ th atom along the  $\mu$ th direction,  $\mathbf{R}_n(l)$  is a lattice translation vector, and  $\omega$  the normal mode frequency. In the harmonic approximation, the equation of motion for the vibration amplitude  $u_{n\mu}$  is

$$\omega^2 u_{n\mu} = \sum_{m,\nu} D_{\mu\nu}(mn, \mathbf{k}) u_{m\nu} + \sum_{\nu} \frac{i\omega B q_n}{m_n} u_{n\nu} \epsilon_{\mu\nu}, \quad (3)$$

where  $\epsilon_{\mu\nu}$  is the  $2d$  Levi-Civita tensor. The element  $D_{\mu\nu}(mn, \mathbf{k})$  of the dynamical matrix reads as

$$D_{\mu\nu}(mn, \mathbf{k}) = - \sum_{l'} \frac{\gamma_{nm}}{\sqrt{m_m m_n}} e_{\mu}(m) e_{\nu}(m) e^{i\mathbf{k} \cdot \mathbf{R}_{nm}(l')}, \quad (4)$$

where  $\hat{e}(m)$  is the unit vector along the translational vector  $\mathbf{R}_{nm}(l')$  connecting the  $m$ th atom in the  $l'$  unit cell to the  $n$ th atom in the  $l = 0$  unit cell, while  $\gamma_{nm} > 0$  is the spring constant between  $n$ th and  $m$ th ions. Plugging Eq. (4) into Eq. (5), we can rewrite the equations of motion as

$$\omega^2 \begin{pmatrix} \mathbf{u}_+ \\ \mathbf{u}_- \end{pmatrix} = \mathcal{A}(\mathbf{k}, \omega) \begin{pmatrix} \mathbf{u}_+ \\ \mathbf{u}_- \end{pmatrix}, \quad (5)$$

where

$$\mathcal{A}(\mathbf{k}, \omega) = \begin{bmatrix} \frac{2\gamma + 2\gamma_1(1 - \cos k_x a \cos k_y a)}{m_+} & \frac{i\omega Z e B - 2\gamma_1 \sin k_x a \sin k_y a}{m_+} & -\frac{2\gamma \cos k_x a}{\sqrt{m_+ m_-}} & 0 \\ -\frac{2\gamma_1 \sin k_x a \sin k_y a + i\omega Z e B}{m_+} & \frac{2\gamma + 2\gamma_1(1 - \cos k_x a \cos k_y a)}{m_+} & 0 & -\frac{2\gamma \cos k_y a}{\sqrt{m_+ m_-}} \\ -\frac{2\gamma \cos k_x a}{\sqrt{m_+ m_-}} & 0 & \frac{2\gamma + 2\gamma_2(1 - \cos k_x a \cos k_y a)}{m_-} & -\frac{2\gamma_2 \sin k_x a \sin k_y a + i\omega Z e B}{m_-} \\ 0 & -\frac{2\gamma \cos k_y a}{\sqrt{m_+ m_-}} & \frac{i\omega Z e B - 2\gamma_2 \sin k_x a \sin k_y a}{m_-} & \frac{2\gamma + 2\gamma_2(1 - \cos k_x a \cos k_y a)}{m_-} \end{bmatrix}, \quad (6)$$

with  $a$  being the lattice constant. In the following, we set  $k_y = 0$  and we focus on the long-wavelength limit of the phonon dynamics by assuming that  $k_x a \ll 1$ . It is convenient to work in the basis of eigenmodes of Eq. (5) for  $k_x = 0$  and  $B = 0$ , which are the in-phase ( $\mathbf{u}_a$ ) and out of phase ( $\mathbf{u}_o$ ) ionic motions,

$$u_{a\mu} = \sqrt{\frac{m_-}{m_- + m_+}} \left( u_{-\mu} + \sqrt{\frac{m_+}{m_-}} u_{+\mu} \right), \quad (7)$$

$$u_{o\mu} = \sqrt{\frac{m_+}{m_- + m_+}} \left( u_{-\mu} - \sqrt{\frac{m_-}{m_+}} u_{+\mu} \right). \quad (8)$$

In this basis, we can rewrite the dynamical matrix (6) as

$$\mathcal{A}(k_x, \omega) = \begin{bmatrix} \frac{(2\gamma+\gamma_1+\gamma_2)(k_x a)^2}{m_++m_-} & 0 & \frac{[m_+(\gamma+\gamma_2)-m_-(\gamma+\gamma_1)](k_x a)^2}{\sqrt{m_+m_-}(m_++m_-)} & -\frac{iZeB\omega}{\sqrt{m_+m_-}} \\ 0 & \frac{(\gamma_1+\gamma_2)(k_x a)^2}{m_++m_-} & \frac{iZeB\omega}{\sqrt{m_+m_-}} & \frac{(m_+\gamma_2-m_-\gamma_1)(k_x a)^2}{\sqrt{m_+m_-}(m_++m_-)} \\ \frac{[m_+(\gamma+\gamma_2)-m_-(\gamma+\gamma_1)](k_x a)^2}{\sqrt{m_+m_-}(m_++m_-)} & -\frac{iZeB\omega}{\sqrt{m_+m_-}} & \frac{2\gamma(m_++m_-)^2+(\gamma_2m_+^2+\gamma_1m_-^2-2\gamma m_+m_-)(k_x a)^2}{m_+m_-(m_++m_-)} & -\frac{iZeB(m_+-m_-)\omega}{m_+m_-} \\ \frac{iZeB\omega}{\sqrt{m_+m_-}} & \frac{(m_+\gamma_2-m_-\gamma_1)(k_x a)^2}{\sqrt{m_+m_-}(m_++m_-)} & \frac{iZeB(m_+-m_-)\omega}{m_+m_-} & \frac{2\gamma(m_++m_-)^2+(m_+^2\gamma_2+m_-^2\gamma_1)(k_x a)^2}{m_+m_-(m_++m_-)} \end{bmatrix}. \quad (9)$$

Equation (9) shows that the in-phase motion is coupled to the out-of-phase motion when either  $k_x$  or  $B$  is nonzero. The longitudinal (transverse) in-phase motion of the cations and anions is coupled to out-of-phase longitudinal (transverse) motion via elastic forces, which vanish as  $k_x \rightarrow 0$ . In contrast the Lorentz force yields a wave vector-independent interaction between the longitudinal in-phase motion and the out-of-phase transverse motion. When the cation and anion have different masses, the Lorentz force also directly couples the transverse and longitudinal out-of-phase motions.

*Phonon Hall viscosity.*—When TRS is broken, the action of a two-dimensional phonon system allows for a non-dissipative Hall viscosity term [25], i.e.,

$$S_H = \int d^2x dt \left[ -\frac{\eta_H}{2} (\nabla^2 u_{ax} \dot{u}_{ay} - \nabla^2 u_{ay} \dot{u}_{ax}) \right]. \quad (10)$$

To make contact with the definition of phonon Hall viscosity  $\eta_H$  introduced in Eq. (10), we derive a low-energy theory for the in-phase modes  $\mathbf{u}_a$  by integrating over out-of-phase modes in the imaginary-time phonon-system action  $\mathcal{S}[\mathbf{u}_a, \mathbf{u}_o]$  corresponding to Eq. (9). The effective action  $\mathcal{S}_a$  for the low-energy nearly in-phase modes is

$$e^{-\mathcal{S}_a[\mathbf{u}_a]} = \int \mathcal{D}\mathbf{u}_o^* \mathcal{D}\mathbf{u}_o e^{-\mathcal{S}[\mathbf{u}_a, \mathbf{u}_o]}. \quad (11)$$

To leading order in the small parameters  $k_x a$  and  $\omega_c/\omega_o$ , the resulting equations of motion are

$$\omega^2 \left[ 1 + \frac{\omega_c^2}{\omega_o^2} \right] u_{ax} = c_l^2 (k_x a)^2 u_{ax} + \frac{i\omega\omega_c [m_+(\gamma+2\gamma_2) - m_-(\gamma+2\gamma_1)] (k_x a)^2}{\omega_o^2 (m_++m_-) \sqrt{m_+m_-}} u_{ay}, \quad (12)$$

$$\omega^2 \left[ 1 + \frac{\omega_c^2}{\omega_o^2} \right] u_{ay} = c_t^2 (k_x a)^2 u_{ay} - \frac{i\omega\omega_c [m_+(\gamma+2\gamma_2) - m_-(\gamma+2\gamma_1)] (k_x a)^2}{\omega_o^2 (m_++m_-) \sqrt{m_+m_-}} u_{ax}. \quad (13)$$

Here,  $\omega_o$  is the optical phonon frequency at the  $\Gamma = (0, 0)$  point,  $\omega_c$  is the cyclotron frequency, and  $c_l$  and  $c_t$  are the longitudinal and transverse phonon velocities:

$$\omega_o = \sqrt{\frac{2\gamma(m_++m_-)}{m_+m_-}}, \quad \omega_c = \frac{Z^* e B}{\sqrt{m_+m_-}}, \\ c_l = \sqrt{\frac{2\gamma+\gamma_1+\gamma_2}{m_++m_-}}, \quad c_t = \sqrt{\frac{\gamma_1+\gamma_2}{m_++m_-}}. \quad (14)$$

The phonon Hall viscosity  $\eta_H$  can be extracted from Eqs. (10), (12), and (13) by identifying  $\rho = a^{-2}(m_++m_-)$  [39]. We find that

$$\eta_H = \frac{\omega_c m_+(\gamma+2\gamma_2) - m_-(\gamma+2\gamma_1)}{\omega_o^2 \sqrt{m_+m_-}}, \\ = \frac{m_+(\gamma+2\gamma_2) - m_-(\gamma+2\gamma_1)}{2\gamma(m_++m_-)} Z^* e B. \quad (15)$$

Equation (15) shows that acoustic phonons in ionic crystals can acquire a dissipationless Hall viscosity whose strength is proportional to the magnetic field. This is the central result of our work.

The strength and sign of the phonon Hall viscosity (15) strongly depends on the ratio  $x = m_-/m_+$  between the mass of cations and anions. For  $x \gg 1$ , the Hall viscosity is negative and approaches the value  $\eta_H \sim -(1/2 + \gamma_1/\gamma)ZeB$ . For  $x = (\gamma+2\gamma_2)/(\gamma+2\gamma_1)\eta_H$  crosses zero, to then increase until it reaches its saturation value  $\eta_H \sim (1/2 + \gamma_2/\gamma)ZeB$  for  $x \ll 1$ . We therefore expect positive Hall viscosities in oxides because their anions are light.

Since the Lorentz force couples transverse and longitudinal motion only when the ion motion is out of phase,

the denominator in Eq. (15) is proportional to  $\omega_o^2$ , instead of  $c_l^2 - c_t^2$ . The role of the phonon force constants is to couple in-phase and out-of-phase motion at finite wave vectors.

Choosing Cu and O as typical cation and anion masses, we take the optical phonon frequency of a  $\text{CuO}_2$  plane, i.e.,  $\omega_0 \sim 2.5$  THz [40], and set  $\gamma_1 \sim \gamma/2$  and  $\gamma_2 \sim 3\gamma/4$ . We find that the typical numerical value of  $\eta_H$  at  $B = 10$  T is  $\sim 5 \times 10^{-18}$   $\text{kg s}^{-1}$ .

The wave equations (12) and (13) explicitly couple longitudinal and transverse phonon modes. We characterize the chirality of acoustic phonon modes by the polarization  $p_a$  defined as the ratio of the transverse to the longitudinal component in the dominantly longitudinal mode. For wave vectors in the  $\hat{x}$  direction  $p_a \equiv |u_{ay}/u_{ax}|$ . From Eqs. (12) and (13),

$$p_a \approx \frac{c_l(k_x a)}{2\gamma} |\eta_H|, \quad (16)$$

at long wavelengths. As shown by the overlapping blue lines in Fig. 2, Eq. (16) is in excellent agreement with the polarization obtained numerically from Eq. (9). However, according to Eq. (16),  $p_a$  is nonzero only if  $\eta_H \neq 0$ , while the polarization  $p_a$  calculated from Eq. (9) vanishes at all wave vectors only when the elastic coupling between the in-phase motion and out-of-phase dynamics vanish entirely, i.e., when  $m_+ = m_-$  and  $\gamma_1 = \gamma_2$ . The more stringent condition for the absence of field-induced coupling between longitudinal and transverse modes is captured when terms of order  $(k_x a)^4 B$  are retained in the low-energy effective model.

Figure 2 additionally displays the dependence of the polarization  $p_o = |u_{oy}/u_{ox}|$  of the out-of-phase longitudinal mode on the magnetic field (orange line). Since

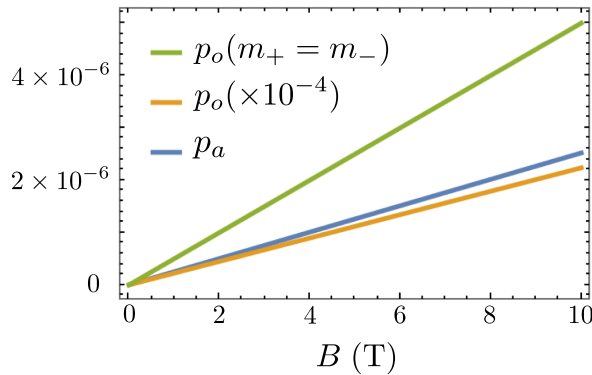


FIG. 2. Blue line: dependence of the polarization  $p_a$  of the longitudinal in-phase mode on the magnetic field, calculated from Eqs. (16) and (9). The two sets of data overlap. Orange and green line: dependence of the polarization  $p_o$  of the longitudinal out-of-phase mode on the magnetic field when choosing Cu and O as cation and anion masses and when setting  $m_+ = m_-$ , respectively. If not otherwise specified, the figures are plotted using the parameters listed in the main text.

Lorentz forces directly couple transverse and longitudinal out-of-phase modes, the polarization of the out-of-phase mode is several order of magnitude larger ( $\sim 10^4$  for our parameters) than the polarization of the in-phase mode. When the Lorentz force coupling the transverse and longitudinal out-of-phase motion vanishes, i.e.,  $\mathcal{A}_{34(43)} = 0$  in Eq. (9), the polarization  $p_o$  is significantly reduced (green line). We find that, however,  $p_o$  does not vanish as long as there is a finite elastic coupling between in-phase and out-of-phase modes ( $\gamma_1 \neq \gamma_2$ ).

In addition to coupling longitudinal and transverse phonons, Lorentz forces also give rise to small changes in acoustic phonon frequencies. To leading order in the parameters  $k_x a$  and  $\omega_c/\omega_o$ , Eqs. (12) and (13) imply that both the longitudinal and transverse phonon frequencies are reduced by a factor of  $1 - \omega_c^2/2\omega_o^2$ . With our parameters, one finds  $\omega_c^2/\omega_o^2 \sim 10^{-9}$ .

*Discussion and conclusions.*—In this Letter, we have derived a low-energy effective model for the lattice vibrations of an ionic crystal subjected to a static magnetic field which accounts for the influence of Lorentz forces. We find that the long-wavelength in-phase lattice dynamics is characterized by a finite phonon Hall viscosity, which implies chiral phonon transport. The Lorentz force contribution to the Hall viscosity is rooted in the coupling between the in-phase motion and out-of-phase motion of cations and anions at finite wave vectors. This mechanism leads to typical values of the phonon Hall viscosity  $\eta_H \sim 5 \times 10^{-18}$   $\text{kg s}^{-1}$  at magnetic field  $B = 10$  T. In comparison Barkeshli *et al.* investigated phonon coupling to a variety of TRS-broken electronic states, and estimated [7] resulting Hall viscosities in the range  $\eta_H \sim 10^{-19}$ – $10^{-15}$   $\text{kg s}^{-1}$ .

Our results apply to layered  $3d$  crystals as well when considering phonons with wave-vector oriented parallel to the  $2d$  layers. In the limit of vanishing interlayer coupling, one could obtain the  $3d$  phonon Hall viscosity simply by redefining  $\eta_H \rightarrow \eta_H/a$ . We use a diatomic square lattice toy model to estimate typical viscosity values. However, our conclusions are not particular to the system analyzed as they rely on two key ingredients that are present in every ionic crystal: (i) a wave vector-dependent coupling between the in-phase and out-of-phase motion of the cations and anions (7), (8), i.e., the eigenvectors of the dynamical matrix (6) at the  $\Gamma$  point; (ii) a wave vector-independent coupling between the magnetic field and the out-of-phase modes. Thus, we anticipate any ionic crystal subjected to an out-of-plane magnetic field to be characterized by a finite phonon Hall viscosity. Our model can be easily generalized to more complex crystalline structures, for which first-principles methodologies can be used to estimate the parameters entering the phonon Hall viscosity (15).

The emergence of the phonon Hall effect in ionic crystals subjected to a static magnetic field has been investigated within a quantum treatment by Agarwalla *et al.* [41].

Our classical approach yields an analytical expression for the Hall viscosity, is more transparent, and provides better insight into the parameters that control its strength, allowing comparisons with other phonon Hall viscosity mechanisms.

Experimentally probing the phonon Hall viscosity has proven to be a challenging task. The renormalization of the long-wavelength acoustic phonon spectrum is far below the resolution limits of conventional spectroscopic probes. Moreover, such measurement would not carry any information about the sign of the Hall viscosity. However, it has been recently shown that a finite phonon Hall viscosity is responsible for circular birefringence of transverse acoustic waves [11]. Thus, it yields an acoustic Faraday rotation that can be probed via acoustic cavity interferometry [42,43]. Another candidate probe is time-dependent x-ray diffraction, which allows us to directly image acoustic phonon modes [44].

Naturally, the phonon Hall viscosity yields chiral phonon transport. In an ionic crystal with no magnetic order or symmetry-broken electronic states one might expect our reported phonon Hall viscosity to be the source of phonon Hall signals. Recently, though, it was shown that scattering on charged defects, which are common in ionic crystals, can also lead to skew scattering [26]. However, the resulting phonon Hall effect is predicted to display a temperature dependence  $\propto T^{-1}$ , in contrast to the  $\propto T^5$  dependence of the signal ascribed to impurity scattering of acoustic phonons with finite Hall viscosity [8], which should make the two signals easily distinguishable. Finally, future work should address the role of phonon anharmonicity.

The authors thank B. Ramshaw, L. Taillefer, M.-E. Boulanger, G. Grissonanche, S. Kivelson, K. Behnia, H. Guo, and D. Juraschek for helpful discussions and experimental motivation for this work. This work was supported by the U.S. Department of Energy, Office of Science, Basic Energy Sciences, under Award No. DE-SC0022106, and by the National Science Foundation under Grant No. NSF DMR-2144086.

---

[1] G. Grissonanche, A. Legros, S. Badoux, E. Lefrancois, V. Zlatko, M. Lizaïre, F. Laliberté, A. Gourgout, J. Zhou, S. Pyon, T. Takayama, H. Takagi, S. Ono, N. Doiron-Leyraud, and L. Taillefer, *Nature (London)* **571**, 376 (2019).  
 [2] M.-E. Boulanger, G. Grissonanche, S. Badoux, A. Allaire, E. Lefrancois, A. Legros, A. Gourgout, M. Dion, C. H. Wang, X. H. Chen, R. Liang, W. N. Hardy, D. A. Bonn, and L. Taillefer, *Nat. Commun.* **11**, 5325 (2020).  
 [3] G. Grissonanche, S. Thériault, A. Gourgout, M.-E. Boulanger, E. Lefrancois, A. Ataei, F. Laliberté, M. Dion, J.-S. Zhou, S. Pyon, T. Takayama, H. Takagi, N. Doiron-Leyraud, and L. Taillefer, *Nat. Phys.* **16**, 1108 (2020).

[4] X. Li, B. Fauqué, Z. Zhu, and K. Behnia, *Phys. Rev. Lett.* **124**, 105901 (2020).  
 [5] L. Chen, M.-E. Boulanger, Z.-C. Wang, F. Tafti, and L. Taillefer, *Proc. Natl. Acad. Sci. U.S.A.* **119**, e2208016119 (2022).  
 [6] J.-Y. Chen, S. A. Kivelson, and X.-Q. Sun, *Phys. Rev. Lett.* **124**, 167601 (2020).  
 [7] M. Barkeshli, S. B. Chung, and X.-L. Qi, *Phys. Rev. B* **85**, 245107 (2012).  
 [8] H. Guo and S. Sachdev, *Phys. Rev. B* **103**, 205115 (2021).  
 [9] R. Samajdar, M. S. Scheurer, S. Chatterjee, H. Guo, C. Xu, and S. Sachdev, *Nat. Phys.* **15**, 1290 (2019).  
 [10] M. Barkeshli, S. B. Chung, and X.-L. Qi, *Phys. Rev. B* **85**, 245107 (2012).  
 [11] T. I. Tügel and T. L. Hughes, *Phys. Rev. B* **96**, 174524 (2017).  
 [12] H. Shapourian, T. L. Hughes, and S. Ryu, *Phys. Rev. B* **92**, 165131 (2015).  
 [13] A. Cortijo, Y. Ferreirós, K. Landsteiner, and M. A. H. Vozmediano, *Phys. Rev. Lett.* **115**, 177202 (2015).  
 [14] S. Heidari, A. Cortijo, and R. Asgari, *Phys. Rev. B* **100**, 165427 (2019).  
 [15] M. Ye, R. M. Fernandes, and N. B. Perkins, *Phys. Rev. Res.* **2**, 033180 (2020).  
 [16] L. Zhang and Q. Niu, *Phys. Rev. Lett.* **112**, 085503 (2014).  
 [17] L. Sheng, D. N. Sheng, and C. S. Ting, *Phys. Rev. Lett.* **96**, 155901 (2006).  
 [18] Y. Kagan and L. A. Maksimov, *Phys. Rev. Lett.* **100**, 145902 (2008).  
 [19] J.-S. Wang and L. Zhang, *Phys. Rev. B* **80**, 012301 (2009).  
 [20] L. Zhang, J. Ren, J.-S. Wang, and B. Li, *Phys. Rev. Lett.* **105**, 225901 (2010).  
 [21] L. Zhang, J. Ren, J.-S. Wang, and B. Li, *J. Phys. Condens. Matter* **23**, 305402 (2011).  
 [22] T. Qin, J. Zhou, and J. Shi, *Phys. Rev. B* **86**, 104305 (2012).  
 [23] E. Thingstad, A. Kamra, A. Brataas, and A. Sudbo, *Phys. Rev. Lett.* **122**, 107201 (2019).  
 [24] M. Ye, L. Savary, and L. Balents, arXiv:2103.04223.  
 [25] Y. Zhang, Y. Teng, R. Samajdar, S. Sachdev, and M. S. Scheurer, *Phys. Rev. B* **104**, 035103 (2021).  
 [26] B. Flebus and A. H. MacDonald, *Phys. Rev. B* **105**, L220301 (2022).  
 [27] X.-Q. Sun, J.-Y. Chen, and S. A. Kivelson, *Phys. Rev. B* **106**, 144111 (2022).  
 [28] H. Guo, D. G. Joshi, and S. Sachdev, *Proc. Natl. Acad. Sci. U.S.A.* **119**, e2215141119 (2022).  
 [29] M. Mori, A. Spencer-Smith, O. P. Sushkov, and S. Maekawa, *Phys. Rev. Lett.* **113**, 265901 (2014).  
 [30] E. M. Lifshitz, A. M. Kosevich, and L. P. Pitaevskii, *Theory of Elasticity*, Course of Theoretical Physics Vol. 7 (Elsevier, Oxford, 1986).  
 [31] D. M. Juraschek, M. Fechner, A. V. Balatsky, and N. A. Spaldin, *Phys. Rev. Mater.* **1**, 014401 (2017).  
 [32] D. M. Juraschek and N. A. Spaldin, *Phys. Rev. Mater.* **3**, 064405 (2019).  
 [33] M. Hamada and S. Murakami, *Phys. Rev. B* **101**, 144306 (2020).  
 [34] R. M. Geilhufe and V. Juričić, S. Bonetti, J.-X. Zhu, and A. V. Balatsky, *Phys. Rev. Res.* **3**, L022011 (2021).

- [35] A. Zabalo, C. E. Dreyer, and M. Stengel, *Phys. Rev. B* **105**, 094305 (2022).
- [36] A. Baydin, F. G. G. Hernandez, M. Rodriguez-Vega, A. K. Okazaki, F. Tay, G. T. Noe II, I. Katayama, J. Takeda, H. Nojiri, P. H. O. Rappl, E. Abramof, G. A. Fiete, and J. Kono, *Phys. Rev. Lett.* **128**, 075901 (2022).
- [37] G. Xiong, H. Chen, D. Ma, and L. Zhang, *Phys. Rev. B* **106**, 144302 (2022).
- [38] M. Basini, M. Pancaldi, B. Wehinger, M. Udina, T. Tadano, M. C. Hoffmann, A. V. Balatsky, and S. Bonetti, [arXiv:2210.01690](https://arxiv.org/abs/2210.01690).
- [39] The mass density  $\rho$  enters via the standard kinetic term in the action, i.e.,  $S_\rho = \frac{1}{2} \int d^2x dt \rho (\dot{u}_{ax}^2 + \dot{u}_{ay}^2)$ .
- [40] R. J. Birgeneau, C. Y. Chen, D. R. Gabbe, H. P. Jenssen, M. A. Kastner, C. J. Peters, P. J. Picone, Tineke Thio, T. R. Thurston, H. L. Tuller, J. D. Axe, P. Boni, and G. Shirane, *Phys. Rev. Lett.* **59**, 1329 (1987).
- [41] B. K. Agarwalla, L. Zhang, J.-S. Wang, and B. Li, *Eur. Phys. J. B* **81**, 197 (2011).
- [42] A. Sytcheva, U. Löw, S. Yasin, J. Wosnitza, S. Zherlitsyn, P. Thalmeier, T. Goto, P. Wyder, and B. Lüthi, *Phys. Rev. B* **81**, 214415 (2010).
- [43] Y. Lee, T. M. Haard, W. P. Halperin, and J. A. Sauls, *Nature (London)* **400**, 431 (1999).
- [44] M. Trigo and D. Reis, *MRS Bull.* **35**, 514 (2010).